



HHS Public Access

Author manuscript

Biomaterials. Author manuscript; available in PMC 2016 September 01.

Published in final edited form as:

Biomaterials. 2015 September ; 64: 108–114. doi:10.1016/j.biomaterials.2015.06.033.

Decellularized skeletal muscle as an *in vitro* model for studying drug-extracellular matrix interactions

Jean W. Wassenaar¹, Gerry R. Boss, MD^{2,*}, and Karen L. Christman, PhD^{1,*}

¹Department of Bioengineering, Sanford Consortium of Regenerative Medicine, University of California, San Diego, 92093 (USA)

²Department of Medicine, University of California, San Diego, 92093 (USA)

Abstract

Several factors can affect drug absorption after intramuscular (IM) injection: drug solubility, drug transport across cell membranes, and drug metabolism at the injection site. We found that potential interactions between the drug and the extracellular matrix (ECM) at the injection site can also affect the rate of absorption post-injection. Using decellularized skeletal muscle, we developed a simple method to model drug absorption after IM injection, and showed that the nature of the drug-ECM interaction could be investigated by adding compounds that alter binding. We validated the model using the vitamin B₁₂ analog cobinamide with different bound ligands. Cobinamide is being developed as an IM injectable treatment for cyanide poisoning, and we found that the *in vitro* binding data correlated with previously published *in vivo* drug absorption in animals. Commercially available ECM products, such as collagen and GelTrex, did not recapitulate drug binding behavior. While decellularized ECM has been widely studied in fields such as tissue engineering, this work establishes a novel use of skeletal muscle ECM as a potential *in vitro* model to study drug-ECM interactions during drug development.

Keywords

ECM; muscle; drug delivery; absorption

Introduction

For some drugs, intramuscular (IM) injection as a delivery route may be advantageous: (i) it eliminates the first-pass effect of oral medications; (ii) it provides for more rapid absorption than subcutaneous injection; and (iii) it is faster and technically simpler than intravenous (IV) injection, allowing for drug administration by non-trained personnel, including self administration [1]. In addition, IM administration is a common parenteral route in veterinary medicine [2]. However, translation of the efficacy of IM drug candidates from *in vitro* data

*co-corresponding authors christman@eng.ucsd.edu, gboss@ucsd.edu.

Publisher's Disclaimer: This is a PDF file of an unedited manuscript that has been accepted for publication. As a service to our customers we are providing this early version of the manuscript. The manuscript will undergo copyediting, typesetting, and review of the resulting proof before it is published in its final citable form. Please note that during the production process errors may be discovered which could affect the content, and all legal disclaimers that apply to the journal pertain.

to *in vivo* results involves additional factors, including absorption from the muscle into circulation. Drug absorption can be affected by a variety of factors including drug hydrophilicity/hydrophobicity, drug movement across biological membranes, and blood perfusion at the injection site [1]. Additionally, we found that drug absorption can also be affected by interactions between the drug and the ECM at the injection site.

The ECM is a complex mixture of proteins and polysaccharides, and constitutes a substantial volume of any tissue or organ [3]. Its biochemical composition and physical structure is tissue dependent [4]; in skeletal muscle, it is composed predominantly of several types of collagen, and numerous glycoproteins and proteoglycans [5]. Tissue decellularization is a strategy increasingly employed in tissue engineering because the resulting ECM scaffold retains the native mixture of macromolecules within a 3D structure. Since ECM composition varies widely across tissues, generation of tissue-specific ECM with the correct diversity and distribution of components is advantageous. We have developed a protocol for decellularizing tissue to create tissue-specific ECM for cell culture [6]. Here, we show that the same method of decellularization, when applied to skeletal muscle, produces an ECM scaffold that can be used to study drug-ECM interactions.

In drug development, many *in vitro* assays exist [7-9] that study the effects of the drug on the cell, and vice versa. While these assays can predict some factors that can influence drug absorption post-IM injection, few models exist to investigate possible interactions of drug candidates with the ECM, which we hypothesized could bind injected drugs and prevent systemic delivery. We decellularized porcine skeletal muscle to assess these interactions, using cobinamide as a model drug. Cobinamide is a new agent being developed as an IM-injectable antidote for cyanide poisoning [10, 11]. Due to the swift onset of the effects of cyanide toxicity, absorption of the antidote from the injection site must be rapid; cobinamide with different bound ligands is absorbed at different rates post IM injection [12]. We found that the altered absorption rates could be attributed to differential cobinamide binding to skeletal muscle ECM. We further demonstrated the utility of decellularized skeletal muscle ECM as a biomaterial to study drug-ECM interactions and predict drug absorption after IM injection with two forms of vitamin B₁₂.

Materials and Methods

All animal experiments were performed according to guidelines established by the Animal Care and Use Program at the University of California, San Diego and the American Association for Accreditation of Laboratory Animal Care, and were approved by the UCSD Institutional Animal Care and Use Committee (A3033-01).

Decellularization of porcine skeletal muscle

Porcine skeletal muscle ECM was prepared similarly to previous descriptions [6]. Briefly, pigs were anesthetized with ketamine (25 mg/kg) and xylazine (2mg/kg), followed by euthanasia with phenobarbital (90 mg/kg). Psoas major muscle was collected immediately post-euthanasia. After removal of adipose and connective tissue, the muscle was cut into ~30 mm³ pieces. The tissue pieces were rinsed with ultrapure water, and then stirred in a 1% (wt/vol) solution of sodium dodecyl sulfate (SDS) in phosphate buffered saline (PBS) for

4-5 d to remove the cellular content; they were then rinsed with a dilute solution of Triton X-100 (10 ppm) for 30 min and water overnight. Tissue pieces were transferred into PBS, and used either within one week when stored at 4 °C, or six months when stored at -80 °C.

Characterization of decellularized skeletal muscle

To confirm that cellular content was removed, ECM pieces were fixed with 10% formalin, embedded in paraffin, and sectioned into 10 µm slices. Hematoxylin and eosin (H&E) and Masson's trichrome staining were performed on the sections to confirm removal of cells and assess preservation of ECM proteins, respectively.

To determine structure of the ECM, the samples were prepared and analyzed for scanning electron microscopy (SEM) as previously described [13]. Briefly, ECM pieces were fixed in 2.5% glutaraldehyde for 2 h and subsequently dehydrated in a series of increasingly concentrated ethanol solutions. Samples were then critical point dried (Leica EM CPD300, Leica, Vienna) on Teflon sample holders with 40 exchange cycles of CO₂ at medium speed and 40% stirring. Filling and heating steps were done at slow speed, and venting was performed at medium speed. Post drying, samples were flash frozen in liquid nitrogen and cut with a razor blade. Samples were adhered to double-sided carbon tabs on aluminum stubs, with newly revealed cross-sections facing up. Mounted samples were then sputter coated (Leica SCD500, Leica, Vienna) with ~6 nm of platinum while being rotated. SEM imaging was performed on a FE-SEM (Sigma VP Zeiss Ltd., Cambridge, UK) at 0.6 keV with 30 µm or 60 µm apertures using the in-lens SE1 detector. For comparison to tissue prior to decellularization, fresh skeletal muscle was prepared and imaged using the same protocol.

To identify proteins present in the ECM, tandem mass spectrometry (MS/MS) was performed as previously described [6]. To quantify the sulfated glycosaminoglycan (sGAG) content of the ECM samples, 1,9-dimethylmethylene blue (DMMB) was used [14]. Lyophilized ECM pieces were digested overnight with 100 µg/mL papain (Sigma-Aldrich, St. Louis, MO) in 0.2 M sodium phosphate buffer (pH 6.4) containing 10 mM EDTA and 5 mM cysteine at 65 °C. The papain digested mixture was added to 32 µg/mL DMMB (Sigma-Aldrich) in 5% ethanol/0.2% formic acid containing 2 mg/mL of sodium formate. The resulting sGAG-DMMB complex was precipitated from solution and then solubilized with 50 mM sodium acetate (pH 6.8) containing 10% 1-propanol and 4 M guanidine hydrochloride. Absorbance of the decomplexed solution of DMMB and sGAGs was measured at 656 nm. sGAG concentration was calculated by calibrating against a heparin standard curve (Sigma-Aldrich).

Generation of Cobinamide, and Ligand Binding to Cobinamide

Cobinamide was produced by base hydrolysis of hydroxocobalamin using cerium hydroxide; the cobinamide product was >95% pure as determined by high performance liquid chromatography [15]. Cobinamide has two ligand binding sites, and, in aqueous solutions, water and hydroxyl groups are bound to the cobalt atom, yielding aquohydroxocobinamide. The water and hydroxyl groups can be replaced by other ligands, e.g., by cyanide yielding dicyanocobinamide, by sulfite yielding sulfitecobinamide, or by nitrite yielding dinitrocobinamide. The affinity (K_a) of each of these three ligands for

cobinamide is very different, ranging over a large log scale: K_a overall for cyanide is $\sim 10^{22} \text{ M}^{-2}$, K_a for sulfite is $\sim 10^{11} \text{ M}^{-1}$, and K_a overall for nitrite is $\sim 10^5 \text{ M}^{-2}$ [overall affinity includes the affinity for each of the two cyanide and nitrite ligands [16]. Thus, cobinamide very readily binds cyanide, becoming saturated with two cyanide groups even at a relatively low cyanide to cobinamide ratio, whereas a much higher nitrite to cobinamide ratio is required to saturate cobinamide with two bound nitrite groups [17]. Saturation with sulfite is intermediate to that of cyanide and nitrite.

Measurement of Drug Absorption to ECM

The ECM pieces were drained of PBS and placed in 24-well plates at $0.5 \pm 0.05 \text{ g/well}$. Cobinamide was dissolved in PBS and 1 mL was added to each well, such that the ECM was completely submerged. Unless otherwise noted, initial starting concentration for cobinamide was 1 mM. As a blank, the same volume of PBS was added to separate wells of ECM pieces to account for any potential absorbance from peptides released from the ECM. At various time points, samples of the solution were taken to measure the cobinamide concentration using a NanoDrop 2000c Spectrophotometer (Thermo Scientific). Peak absorbance for aquohydroxocobinamide, dinitrocobinamide, sulfitecobinamide, and dicyanocobinamide were 346 nm, 349 nm, 320 nm, and 364 nm, respectively. Hydroxocobalamin (HO-Cbl, 354 nm) and cyanocobalamin (CN-Cbl, 363 nm) were also tested. Drug concentration was reported at each time point as a percentage of the initial concentration. For each experiment, ECM water content ($\%_{\text{water}}$) was determined by lyophilizing ECM pieces and measuring the change in weight attributable to water loss. To account for the dilution effect from additional water in the ECM, an adjusted solution concentration (C_{adj}) was calculated at the final time

point by the following formula: $C_{\text{adj}} = C_{\text{meas}} \times \left(1 + \frac{m_{\text{ECM}} \cdot \%_{\text{water}}}{V} \right)$, where C_{meas} is the measured solution concentration (as a percentage of initial concentration), V is the volume of solution added, and m_{ECM} is the mass of the ECM pieces.

To assess the mechanism of cobinamide interaction with the ECM, agents that could alter binding were added with cobinamide, specifically triton (1%), sodium chloride (NaCl, at 100 mM and 1 M), and sodium nitrite (NaNO_2 , at 2, 5, and 10 mEq ratios compared to cobinamide). The cobinamide concentration was measured after the equilibration period and compared to cobinamide alone. An increase in cobinamide concentration would indicate that the added agent reduced binding.

Removal of Sulfates and Glycans

Decellularized ECM was desulfated with Sulfatase Type H-2 aqueous solution (Sigma). Hydrated ECM pieces were weighed and then submerged in 10x volume of sodium acetate at pH 5. An equivolume of 20 U/mL sulfatase in 2 mg/mL NaCl was added to each sample. For control samples, 2 mg/mL NaCl without sulfatase was added. Samples were incubated at 37 °C for 1 hour. Glycans on ECM pieces were also removed using Glycoprofile II, Enzymatic In-Solution N-Glycosylation Kit (Sigma) according to manufacturer's directions. Control samples were treated with water instead of the active PNGase F enzyme. Samples were incubated at 37 °C overnight. After completion of either protocol, ECM pieces were rinsed extensively with PBS, then frozen and lyophilized to measure removal of sulfates and

glycans using the DMMB assay described above. Aquohydroxocobinamide binding to desulfated and deglycosylated ECM pieces, and their respective no-enzyme controls were assessed as described in the previous section.

Hydrogel Formation

Collagen hydrogels were made using rat tail collagen type I (BD Bioscience, San Jose, CA). Collagen type I solubilized in acetic acid (8-11 mg/mL) was brought to pH 7.4 through addition of 1 N sodium hydroxide (NaOH) and 10 × PBS, then diluted to 5 mg/mL with 1 × PBS. Geltrex (Life Technologies, Carlsbad, CA) hydrogels were formed by diluting the matrix solution to 4-6 mg/mL (from starting concentration of 12-19 mg/mL). Skeletal muscle ECM hydrogels were prepared as previously described [6]. Briefly, ECM pieces were lyophilized, milled to a powder, and then digested with 1 mg/mL pepsin (Sigma, St. Louis, MO) and dissolved in 0.1 M HCl. After 48 h, the partially digested ECM mixture was brought to pH 7.4 and 6 mg/mL with NaOH and PBS. All protein mixtures were incubated at 37 °C overnight to allow gelation. Hydrogels of hyaluronic acid (HA), an anionic non-sulfated GAG, were made using methacrylated HA (gift of A. Engler, University of California San Diego), dissolved at 3% w/v in PBS, mixed with 0.05% Irgacure 2959 (BASF Chemical Co., Florham Park, NJ), and then photopolymerized under 350 nm UV light for 5 min. After hydrogel formation, 1 mM cobinamide was added and the change in solution concentration was measured by NanoDrop after 24 h.

To form heparin and chondroitin sulfate conjugated hydrogels, the sulfated GAGs were immobilized onto collagen gels through 1-ethyl-3-(3-dimethylaminopropyl)carbodiimide and N-hydroxysuccinimide (EDC/NHS) conjugation using a modified protocol [18]. As described above, rat tail collagen type I was brought to pH 7.4 at 5 mg/mL concentration. EDC (Oakwood Chemical, West Columbia, SC), NHS (Oakwood Chemical), chondroitin sulfate (Sigma-Aldrich), and heparin were dissolved in 50 mM pH 4.5 MES buffer. Solutions of EDC, NHS, and either chondroitin sulfate or heparin were added to the collagen to final concentrations of 2.5 mg/mL collagen, 24 mM EDC, 5 mM NHS, and 2% w/v chondroitin sulfate or heparin. After gelation at 37 °C overnight, resulting hydrogels were washed several times with PBS to remove unreacted ligands. Control gels of only EDC/NHS, chondroitin sulfate, or heparin were also synthesized in the same manner. After washing, the DMMB assay was used to quantify amount of sGAG conjugation and the different cobinamide species were added to the hydrogels to measure degree of interaction. Similar to analysis with skeletal muscle ECM pieces, water percentage of all hydrogels was measured to calculate percent hydration.

Statistical Analysis

All data are presented as mean ± standard deviation. Samples were measured in triplicate unless otherwise noted. Significance was determined first using a one-way ANOVA followed by either Dunnett's or Tukey's post hoc test. Significance was accepted at $p < 0.05$.

Results

Decellularized Skeletal Muscle Characterization

After completing the decellularization process on porcine skeletal muscle, the ECM pieces were stained with H&E and Masson's trichrome to assess removal of cellular content. Absence of nuclei and contractile proteins in the H&E images indicated decellularization (Fig. 1A). Cross-sections of the muscle fibers showed that the structure of the skeletal muscle ECM was well preserved, with both the perimysium (large arrows) that surrounds the fascicle and the endomysium (small arrows) that surrounds individual muscle fibers identifiable. Masson's Trichrome showed that the major component of the ECM is collagen, which appears blue in this stain (Fig. 1B). Using scanning electron microscopy, we further verified that the native structure of the skeletal muscle ECM was preserved (Fig. 1C). In comparison to cross-sections of fresh skeletal muscle, which have visible myofibrils within each muscle fiber, the decellularized ECM showed only endomysium surrounding the cells (Fig. 1D).

To determine the composition of the skeletal muscle ECM, we performed mass spectrometry (Supplemental Table 1). Consistent with collagen I being the most abundant protein in skeletal muscle ECM [19], collagen I peptides were the most commonly detected peptides in the sample. Types II-VI, XI, XII, XIV, and XXI collagen were also detected as well as elastin and dermatopontin. In addition, common glycoproteins, such as fibronectin and laminin, were found as well as fibrillins-1, -2, emilin-1, and fibulin-5, all of which are involved in elastic fiber formation. Proteoglycans were also detected, specifically lumican (a keratan sulfate proteoglycan) and perlecan (a heparan sulfate proteoglycan of the basement membrane). Since non-proteinaceous GAGs are a major component of the ECM, we measured the sGAG content of the skeletal muscle ECM, and found it to be $7.02 \pm 0.23 \mu\text{g}$ per mg of dry ECM, indicating the decellularization process retained sGAGs.

In vitro Drug-ECM Binding

We previously found that aquohydroxocobinamide is poorly absorbed after IM injection in animals [17], but that both sulfitecobinamide and dinitrocobinamide are well absorbed after IM injection [20]. Aquohydroxocobinamide has two free ligand binding sites, and could be retarded in absorption due to binding to a muscle component more than sulfite- or dinitrocobinamide where the ligand sites are occupied with sulfite and nitrite groups, respectively. To test this hypothesis, we added each of the three cobinamide species to pieces of decellularized skeletal muscle ECM, and measured the cobinamide concentration remaining in solution. We compared results to those obtained using dicyanocobinamide, which would be expected to bind the least to ECM because the cyanide groups bind extremely tightly to cobinamide [17]. On adding cobinamide solutions to the ECM pieces, the concentration of cobinamide detectable in solution decreased rapidly (Fig. 2A). After 4 to 8 hours, the cobinamide concentration reached equilibrium (Fig. 2B). Changes in solution concentration were detectable both visually and by spectroscopy. Notably, the ECM pieces, which initially started out white, became intensely colored by cobinamide, and inversely the cobinamide solution became less saturated (Fig 2D). Upon calculating the adjusted solution concentration (C_{adj}) (Fig. 2C), which takes into account ECM hydration, we found that all of

the added dicyanocobinamide ((CN)₂-Cbi) remained in solution (101.3 ± 6.9%). In contrast, 23.3 ± 1.5% of aquohydroxocobinamide (AH-Cbi), 44.8 ± 4.3 % of dinitrocobinamide ((NO₂)₂-Cbi), and 86.0 ± 0.3% of sulfitocobinamide (SO₃-Cbi) remained in solution. Similar results were obtained using both ECM produced from previously frozen skeletal muscle (Supplemental Fig. 1A) as well as ECM that had been frozen post-decellularization (Supplemental Fig. 1B). These data correlate inversely with the relative affinities of cobinamide for water, nitrite, sulfite, and cyanide, i.e., the lower the affinity of cobinamide for the ligand, the more cobinamide bound to the ECM — and hence the less cobinamide remained in solution. High binding affinity of aquohydroxocobinamide to ECM was further evident when drug-bound ECM pieces were aggressively rinsed with PBS (Supplemental Fig. 2A), with minimal release of aquohydroxocobinamide at a level below spectroscopic detection. In comparison, dicyanocobinamide was washed out from the ECM pieces (Supplemental Fig. 2B).

To study the mechanism of cobinamide binding to ECM, we tested the effects of high salt concentrations (100 mM and 1 M NaCl) and a non-ionic surfactant (1% Triton X-100) on cobinamide binding. We found that neither the salt (Fig. 3A) nor detergent (Fig. 3B) affected cobinamide binding, suggesting that cobinamide was not binding to ECM through either an ionic or hydrophobic interaction. However, we did find that increasing the amount of nitrite added to dinitrocobinamide further reduced cobinamide binding to the ECM (Fig. 3C), suggesting that the nitrite competed with ECM binding sites. To determine whether cobinamide bound to the polysaccharide component, ECM pieces were treated with sulfatase and PNGase F, which removes sulfates on sGAGs and N-linked glycosylation, respectively. Quantification of remaining sGAG content using DMMB showed that sulfatase treatment removed 89 ± 3% while PNGase F removed 23 ± 7% of the original sGAGs of decellularized ECM. Aquohydroxocobinamide binding to both treated ECMs was measured; however, there were no significant differences compared to non-enzyme controls (Supplemental Fig. 3).

To further test the decellularized skeletal muscle ECM as a platform for studying drug-ECM interactions, we tested two forms of vitamin B₁₂, i.e., hydroxocobalamin and cyanocobalamin, which are injected IM to treat vitamin B₁₂ deficiency. Cyanocobalamin (CN-Cbl) is more rapidly absorbed post injection than hydroxocobalamin (HO-Cbl), and, like cobinamide, hydroxocobalamin binds cyanide much more tightly than it binds water or hydroxyl molecules [21, 22]. Consistent with these previous reports, we found minimal binding of cyanocobalamin to ECM and moderate binding of hydroxocobalamin, with C_{adj} of 101.4 ± 0.3 % and 49.1 ± 1.4 %, respectively (Fig. 4).

Decellularized ECM Provides the Optimal Platform for Studying Drug-ECM Interactions

To determine whether intact decellularized ECM was necessary to study drug-ECM interactions, we tested cobinamide binding to both simple ECM mimics as well as commercially available ECMs. Since collagen is widely used for cell culture applications, readily forms a hydrogel, and is the predominant component of skeletal muscle ECM [5], we first tested type I collagen hydrogels. After adjusting for hydrogel hydration, we found almost all of the aquohydroxocobinamide, nitrocobinamide, sulfitocobinamide, and

dicyanocobinamide in solution, demonstrating lack of binding (Fig. 5). We also sought to establish the ECM component that bound cobinamide by using collagen hydrogels conjugated with heparin or chondroitin sulfate, as well as hyaluronic acid (HA) hydrogels. We found no binding of any of the four cobinamide species to these fabricated hydrogels (Supplemental Fig. 4). To assess if cobinamide would bind to a more complex ECM, we tested Geltrex®, a commercially available ECM product similar to Matrigel® that is extracted from murine sarcomas. We also tested hydrogels derived from partial pepsin digestion of skeletal muscle ECM [6]. Cobinamide binding to both Geltrex® and skeletal muscle ECM hydrogels was negligible (Fig. 5).

Discussion

The absorption profile from the injection site of an IM administered drug can have a substantial impact on the drug's therapeutic efficacy. Many factors can affect IM absorption [23, 24], but binding to the ECM is rarely considered. While binding to ECM proteins and GAGs has been proposed, few studies have reported clinically observed ECM-drug interactions [25]. Here, we show that drugs can bind to decellularized ECM, and that a high degree of binding correlates with previously published data showing slow *in vivo* absorption after IM injection [17].

When injected intravenously in cyanide-poisoned animals, aquohydroxocobinamide is far better at rescuing animals than hydroxocobalamin [10]. However, IM injected aquohydroxocobinamide has not been effective due to poor absorption, and when the injection site was examined, a large amount of the cobinamide could be seen in the muscle [17]. Injecting dinitrocobinamide or sulfitecobinamide markedly improved absorption, and we hypothesized this was due to less binding of dinitrocobinamide or sulfitecobinamide than of aquohydroxocobinamide to the skeletal muscle ECM. To test this hypothesis, we added several different liganded cobinamide species to decellularized skeletal muscle ECM, and showed that binding of the different species to the ECM *in vitro* recapitulated the *in vivo* absorption results. Nitrite, sulfite, and cyanide are increasingly stronger ligands for cobinamide, and binding of the respective cobinamide species to the ECM correlated inversely with the ligands' affinity for cobinamide. Thus, we hypothesize that the ligands act as counterions to compete with ECM binding, where higher affinity between the ligand and cobinamide causes less available free cobinamide to bind ECM. Addition of sodium nitrite to dinitrocobinamide led to a dose-dependent decrease of ECM binding, further suggestive of competitive inhibition.

We also found the same phenomena for hydroxocobalamin and cyanocobalamin, which are used to treat vitamin B₁₂ deficiency. Cyanocobalamin is rapidly absorbed from IM sites of injection with plasma concentrations peaking within 1 h of injection, and the majority of the drug excreted in the urine within the first 8 h post-injection [21]. In contrast, hydroxocobalamin is absorbed more slowly, with only half of the dose absorbed in the first 2.5 h and longer excretion over 3 d [22]. We found that cyanocobalamin bound minimally to the ECM *in vitro* while hydroxocobalamin exhibited moderate binding. Interactions with the ECM could therefore explain the difference in pharmacokinetics between the two drugs.

To the best of our knowledge, only one group has previously examined potential ECM-drug interactions. Zhang *et al.* [26] published a method for studying the interaction by using Matrigel®, a commercially available solubilized basement membrane derived from the Engelbreth-Holm-Swarm mouse sarcoma cell line. Subsequently, they applied Matrigel as an ECM mimetic and Comparative Molecular Field Analysis to determine the nature of ECM binding for a series of matrix metalloproteinase (MMP) inhibitors [27]. While Zhang *et al.* applied their method to GM6001 (galardin, ilomastat) [27], a broad range MMP inhibitor most often used clinically in anti-aging creams, no correlation was made between the degree of predicted ECM binding and *in vivo* data. We show that simple ECM mimics and commercially available ECMs, similar to Matrigel®, are not sufficient. Specifically, cobinamide did not bind to hydrogels fabricated with defined components such as collagen type I, heparin, chondroitin sulfate, or HA. To determine whether binding occurred with the polysaccharide components of ECM, we removed glycans as well as sulfates from sGAGs. Neither had a significant effect on reduction of cobinamide binding, indicating that binding could be towards the proteinaceous portion of ECM. This result is however not conclusive since DMMB did not detect complete removal, and there are likely other polysaccharide species that are unaffected by these enzymes. Nevertheless, this approach represents one method for determining the ECM component to which drug binding occurs, by selectively removing ECM components through specific enzymes or blocking antibodies.

Cobinamide may bind to other specific ECM components that we did not examine. Alternatively, binding could occur with the native conformation of ECM components in the decellularized tissue, but not in fabricated hydrogels. For example, type I collagen was extracted from rat tails using acetic acid solubilization, a process that disrupts the ultrastructure of the collagen fibrils [28]. Similarly, EDC/NHS coupling of heparin to poloxamer also changes heparin conformation [29], and EDC modified heparin exhibits loss of anticoagulant activity and susceptibility to heparinase degradation [30]. Cobinamide also did not bind to GelTrex®, a commercially available ECM product similar to Matrigel®. While Matrigel® and Geltrex® approximate ECM in their complexity of proteins and GAGs, their composition more closely resembles the basement membrane of a tumor, consisting primarily of laminin and collagen IV [31], than the ECM of any healthy tissue. In the case of IM injectable drugs, use of ECM decellularized from skeletal muscle should better predict potential binding, since its biochemical composition more faithfully reproduces the injection site. In addition, decellularization also helps maintain the intrinsic structure of ECM. Histological staining and SEM analysis of decellularized skeletal muscle show preservation of fresh skeletal muscle ECM organizational hierarchy with the arrangement of perimysium and endomysium still readily identifiable. Hydrogels derived from skeletal muscle ECM, using a previously developed method [6], did not retain cobinamide. The process of forming the hydrogel involves partial digestion of the ECM proteins with pepsin in an acidic environment. The result is that the ultrastructure of the hydrogel, as assessed using SEM [32] is different from that of native skeletal muscle ECM. Taken collectively, these results further emphasized the importance of using a biomaterial that fully represents the complex mixture of proteins and polysaccharides of the ECM as well as preserves their native conformations, a characteristic that decellularized ECM uniquely possesses for studying drug-ECM interactions.

Drug binding to serum proteins, such as plasma albumin and α -acid glycoprotein, is an often-used strategy (and sometimes unwanted side effect) to attenuate therapeutic action by controlling the free drug concentration in plasma [33]. Similarly, binding to the ECM may also be employed to tune the pharmacokinetics of the drug. In cases where rapid onset of therapeutic action is desired, minimal ECM interaction is necessary; whereas if a prolonged drug effect is desired, high affinity for the ECM with slow release may be preferred. In this study, we demonstrate how the use of decellularized ECM may aid in developing IM injectable drugs. Once ECM binding has been studied, it will likely be important to understand the mechanisms by which this occurs. Each individual drug may have different binding mechanisms, and use of decellularized ECM can be adapted to investigate the mechanism. Since this is a simple to use *in vitro* model, many approaches can be used study this interaction, including those described in this study. Importantly, agents that change binding affinity provide indications of the mechanism and suggest further modifications on the drug formulation for tailoring optimal IM adsorption.

Conclusions

We have demonstrated that decellularized skeletal muscle ECM can be used as an *in vitro* material to study interactions between a drug and ECM. Importantly, only the intact decellularized ECM was able to recapitulate the drug-ECM interaction unlike commercially available ECM mimics such as collagen or GelTrex®. Although we were unable to define the specific mechanisms of cobinamide binding to ECM, the methods used in this study provide a range of approaches for the investigation of ECM binding for other compounds. Since this *in vitro* model is simple to establish, and can even use frozen ECM, it is a novel and convenient method for studying potential drug-ECM interactions for development of IM injectable drugs.

Supplementary Material

Refer to Web version on PubMed Central for supplementary material.

Acknowledgements

This research is funded by NIH 1R01HL113468 and U01NS058030. JWW was supported by pre-doctoral fellowships from the California Institute for Regenerative Medicine and the American Heart Association, as well as the University of California, San Diego Medical Scientist Training Program T32 GM007198-40. We gratefully acknowledge technical assistance in scanning electron microscopy imaging and sample preparation from Matthew Joens and James Fitzpatrick from the Salk Institute Waitt Advanced Biophotonics Center, which is supported by the Waitt Foundation, the W.M. Keck Foundation, NCI (CA014195-41) and NINDS (NS072031-04A1).

References

1. Buxton, ILO. Pharmacokinetics and Pharmacodynamics. In: Brunton, LL., editor. Goodman and Gilman's The Pharmacological Basis of Therapeutics. McGraw-Hill: 2006.
2. Turner PV, Brabb T, Pekow C, Vasbinder MA. Administration of Substances to laboratory animals: routes of administration and factors to consider. J Am Assoc Lab Anim Sci. 2011; 50:600–13. [PubMed: 22330705]
3. Alberts, B.; Johnson, A.; Lewis, J.; Raff, M.; Roberts, K.; Walter, P. Molecular Biology of the Cell. Garland Science; New York, NY: 2008. The extracellular matrix of animal connective tissues.

4. Frantz C, Stewart KM, Weaver VM. The extracellular matrix at a glance. *J Cell Sci.* 2010; 123:4195–200. [PubMed: 21123617]
5. Gillies AR, Lieber RL. Structure and function of the skeletal muscle extracellular matrix. *Muscle Nerve.* 2011; 44:318–31. [PubMed: 21949456]
6. Dequach JA, Mezzano V, Miglani A, Lange S, Keller GM, Sheikh F, et al. Simple and high yielding method for preparing tissue specific extracellular matrix coatings for cell culture. *PLoS ONE.* 2010; 5:e13039. [PubMed: 20885963]
7. Lipinski CA, Lombardo F, Dominy BW, Feeney PJ. Experimental and computational approaches to estimate solubility and permeability in drug discovery and development settings. *Adv Drug Delivery Rev.* 2012; 64:4–17. Supplement.
8. Giacomini KM, Huang S-M, Tweedie DJ, Benet LZ, Brouwer KLR, Chu X, et al. Membrane transporters in drug development. *Nat Rev Drug Discov.* 2010; 9:215–36. [PubMed: 20190787]
9. Dambach DM, Andrews BA, Moulin F. New technologies and screening strategies for hepatotoxicity: Use of in vitro models. *Toxicol Pathol.* 2005; 33:17–26. [PubMed: 15805052]
10. Lee J, Mohammad O, Brenner M, Mahon SB, Sharma VS, Kim J, et al. Comparison of cobinamide to hydroxocobalamin in reversing cyanide physiologic effects in rabbits using diffuse optical spectroscopy monitoring. *J Biomed Opt.* 2010; 15:17001–8.
11. Chan A, Balasubramanian M, Blackledge W, Mohammad OM, Alvarez L, Boss GR, et al. Cobinamide is superior to other treatments in a mouse model of cyanide poisoning. *Clin Toxicol.* 2010; 48:709–17.
12. Brenner M, Kim JG, Mahon SB, Lee J, Kreuter KA, Blackledge W, et al. Intramuscular Cobinamide Sulfite in a Rabbit Model of Sublethal Cyanide Toxicity. *Ann Emerg Med.* 2010; 55:352–63. [PubMed: 20045579]
13. Grover GN, Rao N, Christman KL. Myocardial matrix–polyethylene glycol hybrid hydrogels for tissue engineering. *Nanotechnology.* 2014; 25:014011. [PubMed: 24334615]
14. Barbosa I, Garcia S, Barbier-Chassefière V, Caruelle J-P, Martelly I, Papy-García D. Improved and simple micro assay for sulfated glycosaminoglycans quantification in biological extracts and its use in skin and muscle tissue studies. *Glycobiology.* 2003; 13:647–53. [PubMed: 12773478]
15. Blackledge WC, Blackledge CW, Griesel A, Mahon SB, Brenner M, Pilz RB, et al. New Facile Method to Measure Cyanide in Blood. *Anal Chem.* 2010; 82:4216–21. [PubMed: 20420400]
16. Pratt, JM. *Inorganic Chemistry of Vitamin B12.* Academic Press; New York: 1972.
17. Chan A, Jiang J, Fridman A, Guo LT, Shelton GD, Liu M-T, et al. Nitrocobinamide, a New Cyanide Antidote That Can Be Administered by Intramuscular Injection. *J Med Chem.* 2015; 58:1750–9. [PubMed: 25650735]
18. Pieper JS, Hafmans T, Veerkamp JH, van Kuppevelt TH. Development of tailor-made collagen–glycosaminoglycan matrices: EDC/NHS crosslinking, and ultrastructural aspects. *Biomaterials.* 2000; 21:581–93. [PubMed: 10701459]
19. Purslow, PP. *The Extracellular Matrix of Skeletal and Cardiac Muscle.* Fratzl, P., editor. Springer US; Collagen: 2008. p. 325-57.
20. Brenner M, Benavides S, Mahon SB, Lee J, Yoon D, Mukai D, et al. The vitamin B12 analog cobinamide is an effective hydrogen sulfide antidote in a lethal rabbit model. *Clin Toxicol.* 2014; 52:490–7.
21. American Regent Inc. Cyanocobalamin injection, solution. National Library of Medicine; Bethesda (MD): May. 2008 Available from: <http://dailymed.nlm.nih.gov/dailymed/lookup.cfm?setid=2fb653d6-e2b2-4969-831b-c0dc37b9c0cc>
22. Watson Pharma Inc. Hydroxocobalamin injection, solution. National Library of Medicine; Bethesda (MD): Jul. 2010 Available from: <http://dailymed.nlm.nih.gov/dailymed/lookup.cfm?setid=a3087a39-f218-4f16-a1e7-17c39bb2eb69>
23. Zuidema J, Kadir F, Titulaer HAC, Oussoren C. Release and absorption rates of intramuscularly and subcutaneously injected pharmaceuticals (II). *Int J Pharm.* 1994; 105:189–207.
24. Zuidema J, Pieters F, Duchateau G. Release and absorption rate aspects of intramuscularly injected pharmaceuticals. *Int J Pharm.* 1988; 47:1–12.
25. Saltzman, MW. *Drug Modification.* In: Saltzman, MW., editor. *Drug Delivery: Engineering Principles for Drug Therapy.* 1. Oxford University Press; New York, USA: 2001.

26. Zhang Y, Lukacova V, Reindl K, Balaz S. Quantitative characterization of binding of small molecules to extracellular matrix. *J Biochem Biophys Methods*. 2006; 67:107–22. [PubMed: 16516301]
27. Zhang Y, Lukacova V, Bartus V, Nie X, Sun G, Manivannan E, et al. Binding of Matrix Metalloproteinase Inhibitors to Extracellular Matrix: 3D-QSAR Analysis. *Chem Bio Drug Des*. 2008; 72:237–48. [PubMed: 18844670]
28. Silver FH, Trelstad RL. Type I collagen in solution. Structure and properties of fibril fragments. *J Biol Chem*. 1980; 255:9427–33. [PubMed: 7410433]
29. Zhao Y-Z, Lv H-F, Lu C-T, Chen L-J, Lin M, Zhang M, et al. Evaluation of a Novel Thermosensitive Heparin-Poloxamer Hydrogel for Improving Vascular Anastomosis Quality and Safety in a Rabbit Model. *PLoS ONE*. 2013; 8:e73178. [PubMed: 24015296]
30. Oliveira GB, Carvalho LB Jr, Silva MPC. Properties of carbodiimide treated heparin. *Biomaterials*. 2003; 24:4777–83. [PubMed: 14530075]
31. Kleinman HK, McGarvey ML, Hassell JR, Star VL, Cannon FB, Laurie GW, et al. Basement membrane complexes with biological activity. *Biochemistry*. 1986; 25:312–8. [PubMed: 2937447]
32. DeQuach JA, Lin JE, Cam C, Hu D, Salvatore MA, Sheikh F, et al. Injectable skeletal muscle matrix hydrogel promotes neovascularization and muscle cell infiltration in a hindlimb ischemia model. *Eur Cells Mater*. 2012; 23:400.
33. Trainor, GL. Chapter 31 Plasma Protein Binding and the Free Drug Principle: Recent Developments and Applications. In: John, EM., editor. *Annual Reports in Medicinal Chemistry*. Vol. 42. Academic Press; 2007. p. 489-502.

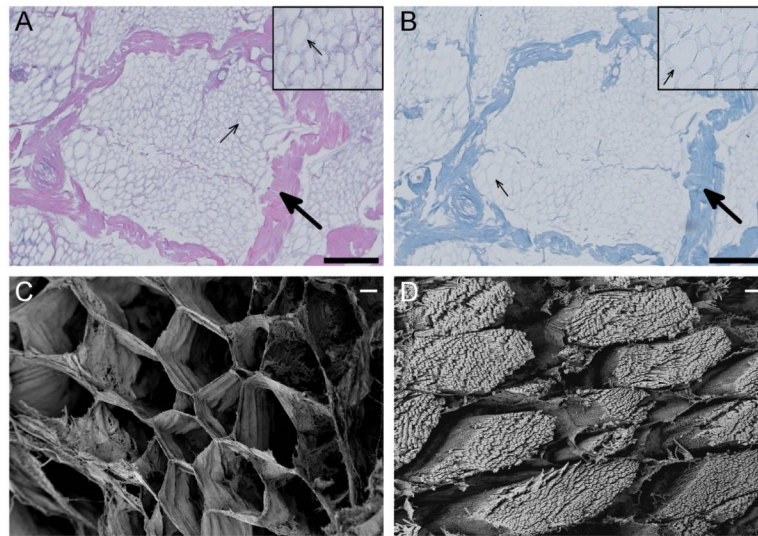


Figure 1. Decellularization confirmation. Histology images taken at 20x of H&E (A) and Masson's trichrome (B) staining of decellularized skeletal muscle shows preservation of ECM architecture, with perimysium (large arrows) and endomysium (small arrows) identifiable (scale bars are 200 µm). Scanning electron images at 500x comparing fresh (C) and decellularized (D) skeletal muscle shows preservation of the honeycomb-like endomysium, while cellular content of the muscle fiber is removed during decellularization (scale bars are 10 µm).

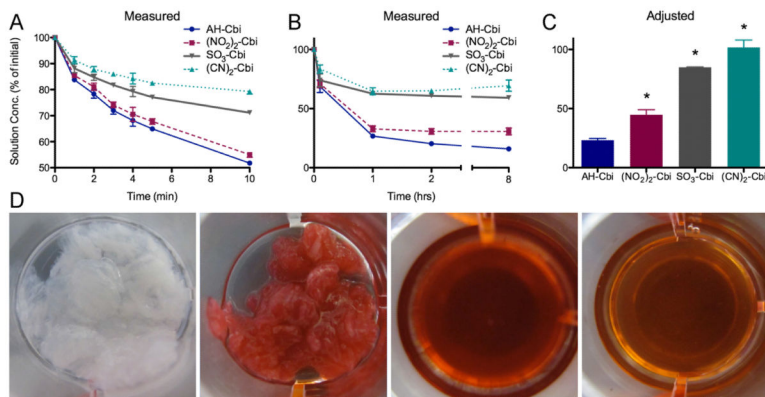


Figure 2. Cobinamide binding to skeletal muscle ECM. Cobinamide concentration as a percentage of initial solution concentration measured by NanoDrop within the first 10 minutes (A) and over 8 hours (B). C) Concentration of the final time point of 8 hours after adjusting for dilution effect from hydrated ECM. Decreased concentration is indicative of greater binding to ECM (* $p < 0.05$ compared to AH-Cbi). D) Visual changes as a result of cobinamide binding going from left to right: 1) decellularized skeletal muscle ECM pieces, 2) ECM pieces removed after 8 hours in 3) 1 mM aquohydroxocobinamide (AH-Cbi) solution, 4) AH-Cbi solution after ECM is removed.

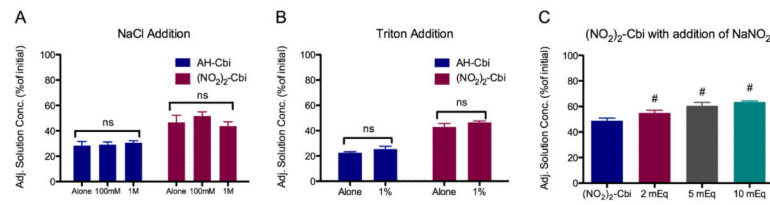


Figure 3.

Effect of ligand, salt, and detergent on cobinamide binding to ECM. Adjusted cobinamide concentration after equilibration for aquohydroxocobinamide (AH-Cbi) and dinitrocobinamide ((NO₂)₂-Cbi) with A) addition of sodium chloride, B) addition of Triton X-100. (#, $p < 0.05$ compared to (NO₂)₂-Cbi), and C) addition of increasing amounts of sodium nitrite to ((NO₂)₂-Cbi).

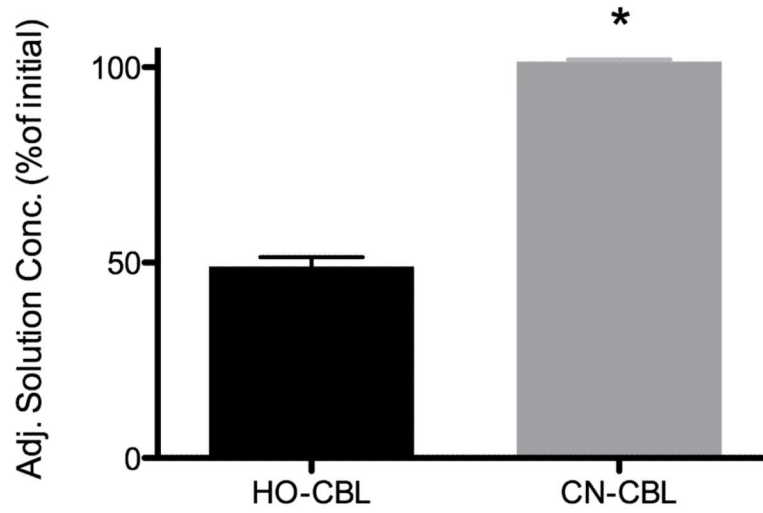


Figure 4. Cobalamin binding to skeletal muscle ECM. Adjusted solution concentration of hydroxocobalamin (HO-Cbl) and cyanocobalamin (CN-Cbl) after 8-hour equilibration with skeletal muscle ECM. (* $p < 0.05$)

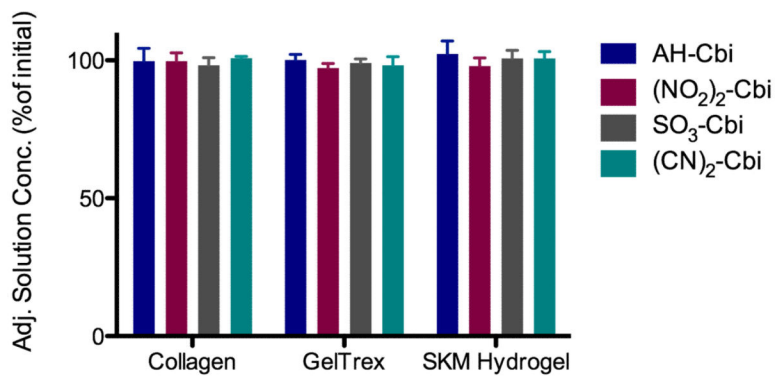


Figure 5. Cobinamide does not bind to other ECM mimics. Adjusted solution concentration of aquohydroxocobinamide (AH-Cbi), dinitrocobinamide ((NO₂)₂-Cbi), sulfitocobinamide (SO₃-Cbi), and dicyanocobinamide ((CN)₂-Cbi) after 8-hour equilibration with ECM derived hydrogels – collagen, Geltrex, and skeletal muscle (SKM) hydrogel. No significant change in solution concentration was detected.